Supporting Figures for: Evaluating the State-of-the-Art in Remote Volcanic Eruption Characterization Part II: Ulawun Volcano, Papua New Guinea

Kathleen McKee (0000-0003-3189-9189)[1], Cassandra Smith (0000-0003-2653-4249)[2], Kevin Reath (0000-0003-1843-8046)[3], Eveanjelene Snee (0000-0002-3660-4020)[4], Sean Maher (0000-0002-9803-916X)[5], Robin S. Matoza (0000-0003-4001-061X)[5], Simon Carn (0000-0002-0360-6660)[6], Larry Mastin (0000-0002-4795-1992)[7], Kyle Anderson (0000-0001-8041-3996)[8], David Damby (0000-0002-3238-3961)[8], Diana Roman (0000-0003-1282-5803)[1], Ima Itikarai ()[9], Kila Mulina ()[9], Steve Saunders ()[9], Jelle Assink (0000-0002-4990-6845)[10], Rodrigo de Negri Leiva (0000-0003-1283-2579)[5,11], Anna Perttu (0000-0003-3590-1549)[12]

[1]Earth and Planets Laboratory, Carnegie Institution for Science, Washington, DC, USA, [2]Alaska Volcano Observatory, Anchorage, AK, USA, [3]Department of Earth and Atmospheric Sciences, Cornell University, Ithaca, NY, USA, [4]School of Earth and Ocean Sciences, Cardiff University, Cardiff, Wales, UK, [5]Department of Earth Science and Earth Research Institute, University of California, Santa Barbara, Santa Barbara, CA, USA, [6]Department of Geological and Mining Engineering and Sciences, Michigan Technological University, Houghton, MI, USA, [7]U.S.Geological Survey Cascades Volcano Observatory, Vancouver, WA, USA, [8]U.S. Geological Survey, California Volcano Observatory, Moffett Field, CA, USA, [9]Rabaul Volcano Observatory, Department of Mining and Petroleum, Geological Survey of Papua New Guinea, Rabaul, Papua New Guinea, [10]R&D Seismology and Acoustics Department, Royal Netherlands Meteorological Institute (KNMI), De Bilt, Netherlands, [11]NDC-CTBT of the Chilean Nuclear Energy Commission, Chile, [12]Earth Observatory of Singapore, Nanyang Technological University, Singapore

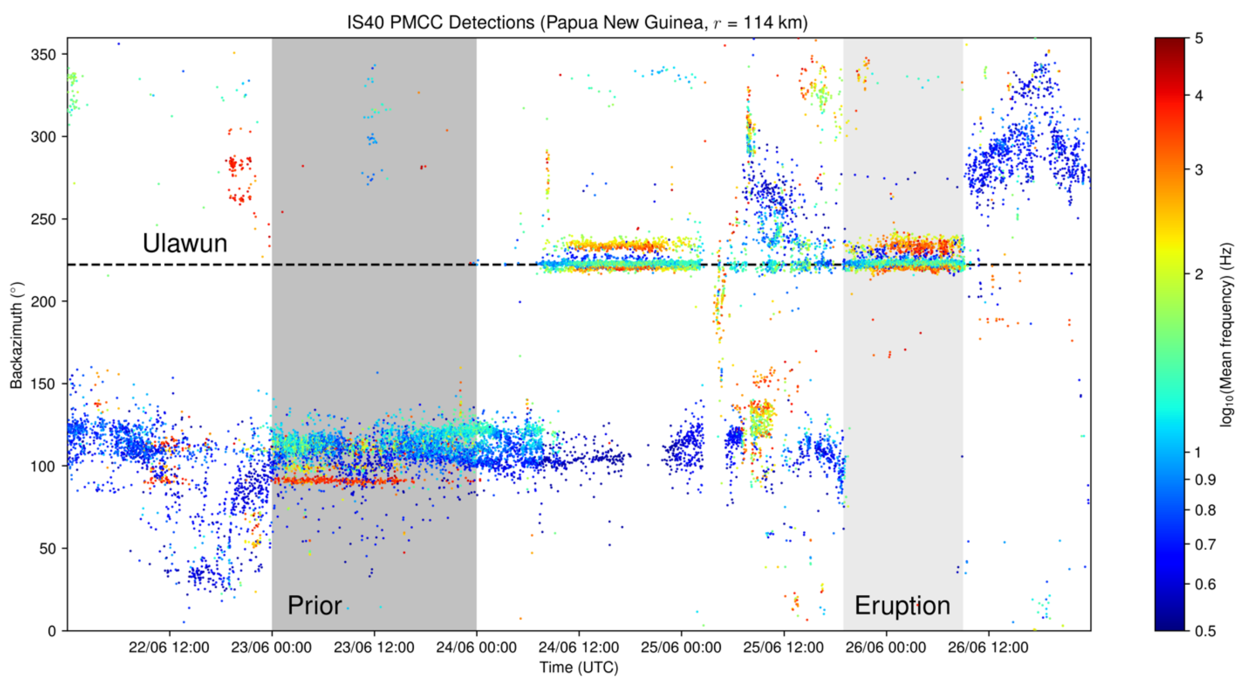

Sup. Fig. 1 - PMCC array processing results from IS40 (Papua New Guinea) for the Ulawun eruption showing the back-azimuths of coherent detections over time. Colors represent the mean frequency of the detection. Dashed line at 33° shows the backazimuth to Ulawun volcano. The shaded "Eruption" region (2019-06-25T19:00:00 to 2019-06-26T09:00:00 UTC) represents the time interval used to locate the main phase of the eruption with IMS_vASC. The shaded "Prior" region (2019-06-23T00:00:00 to 2019-06-24T00:00:00 UTC) represents the time interval used to clean the IMS_vASC grid of detection clutter from ambient noise (see Matoza et al., (2017) for method details).

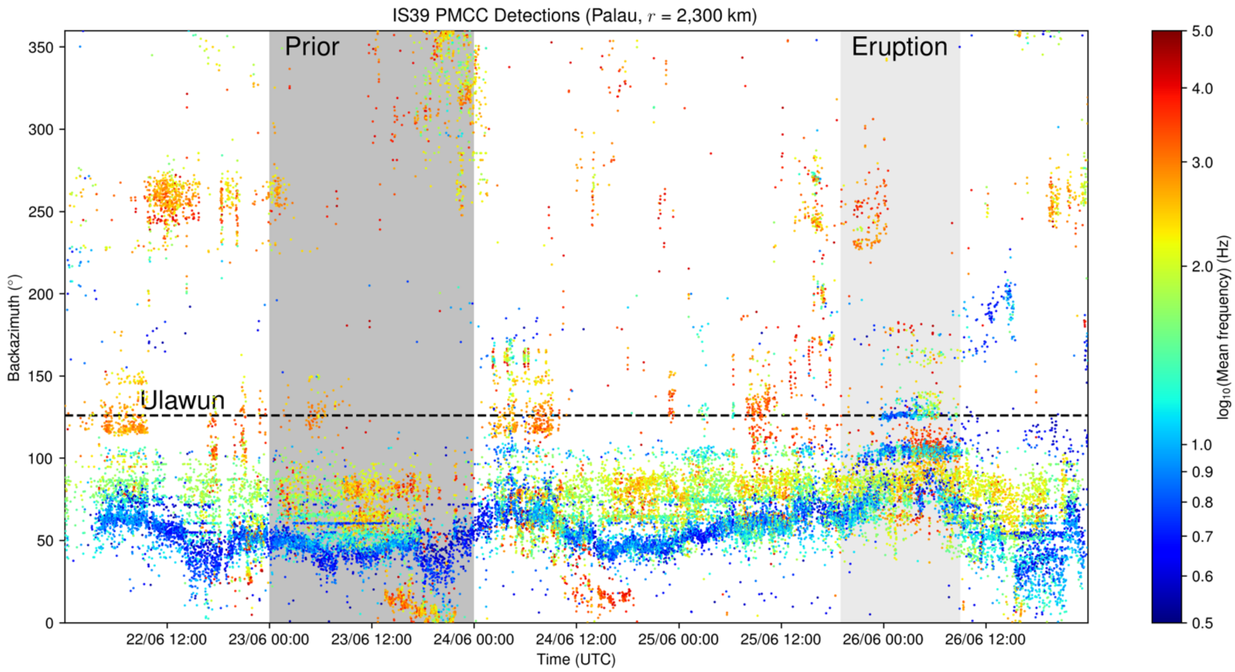

Sup. Fig. 2 - PMCC array processing results from IS39 (Palau) for the Ulawun eruption showing the back-azimuths of coherent detections over time. Colors represent the mean frequency of the detection. Dashed line at 126° shows the backazimuth to Ulawun volcano. The shaded "Eruption" region (2019-06-25T19:00:00 to 2019-06-26T09:00:00 UTC) represents the time interval used to locate the main phase of the eruption with IMS_vASC. The shaded "Prior" region (2019-06-23T00:00:00 to 2019-06-24T00:00:00 UTC) represents the time interval used to clean the IMS_vASC grid of detection clutter from ambient noise (see Matoza et al., (2017) for method details).

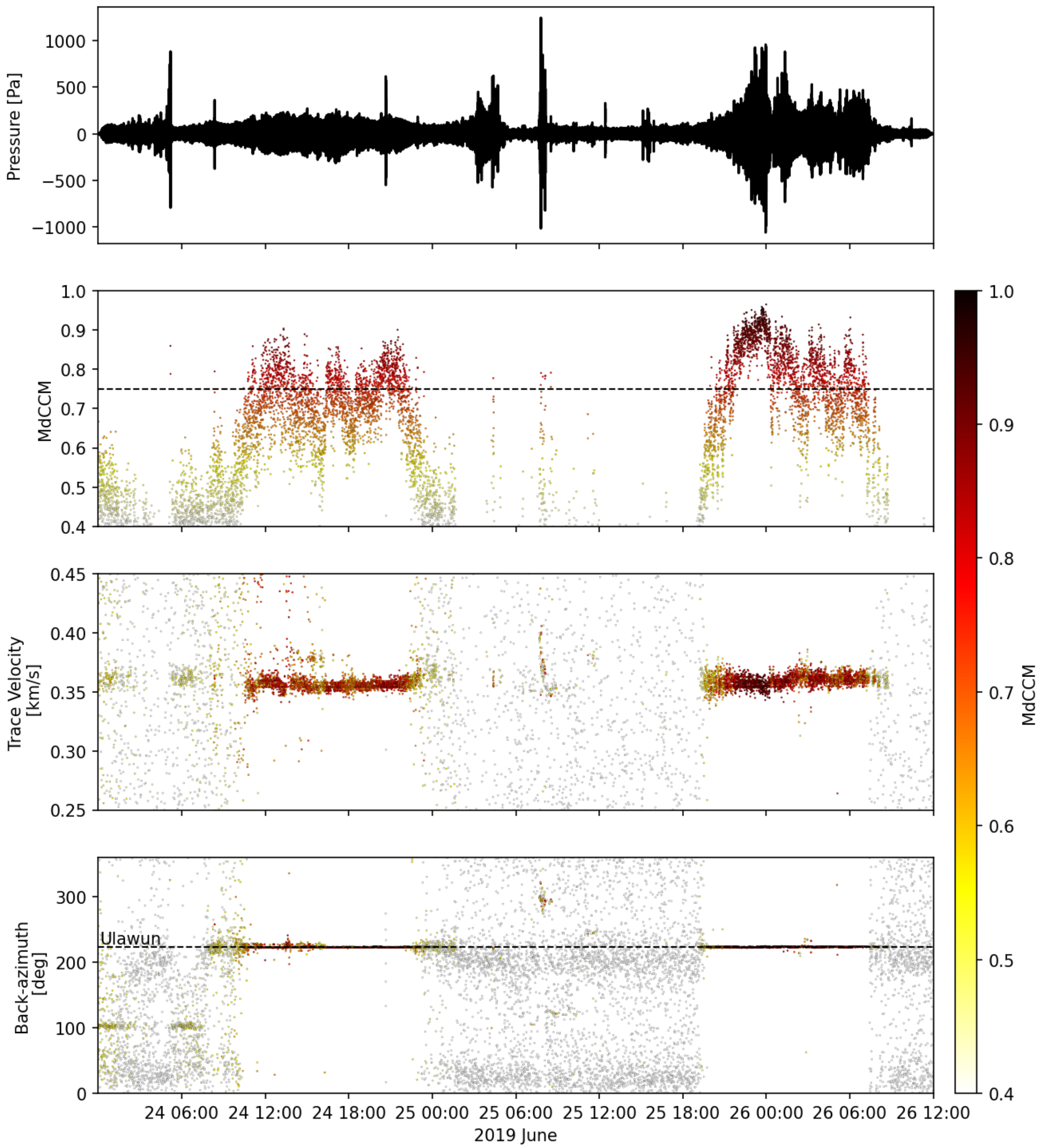

Sup. Fig. 3 - IS40 MdCCM array detection results Ulawun for 24 June at 00:00 to 26 June at 12:00 UTC, data filtered from 0.5 to 5.0 Hz. Top: Best beam of infrasound; 2nd: MCCM, mean cross correlation maximum; 3rd: Estimated trace velocity for each time window; Bottom: Estimated back-azimuth for each time window.

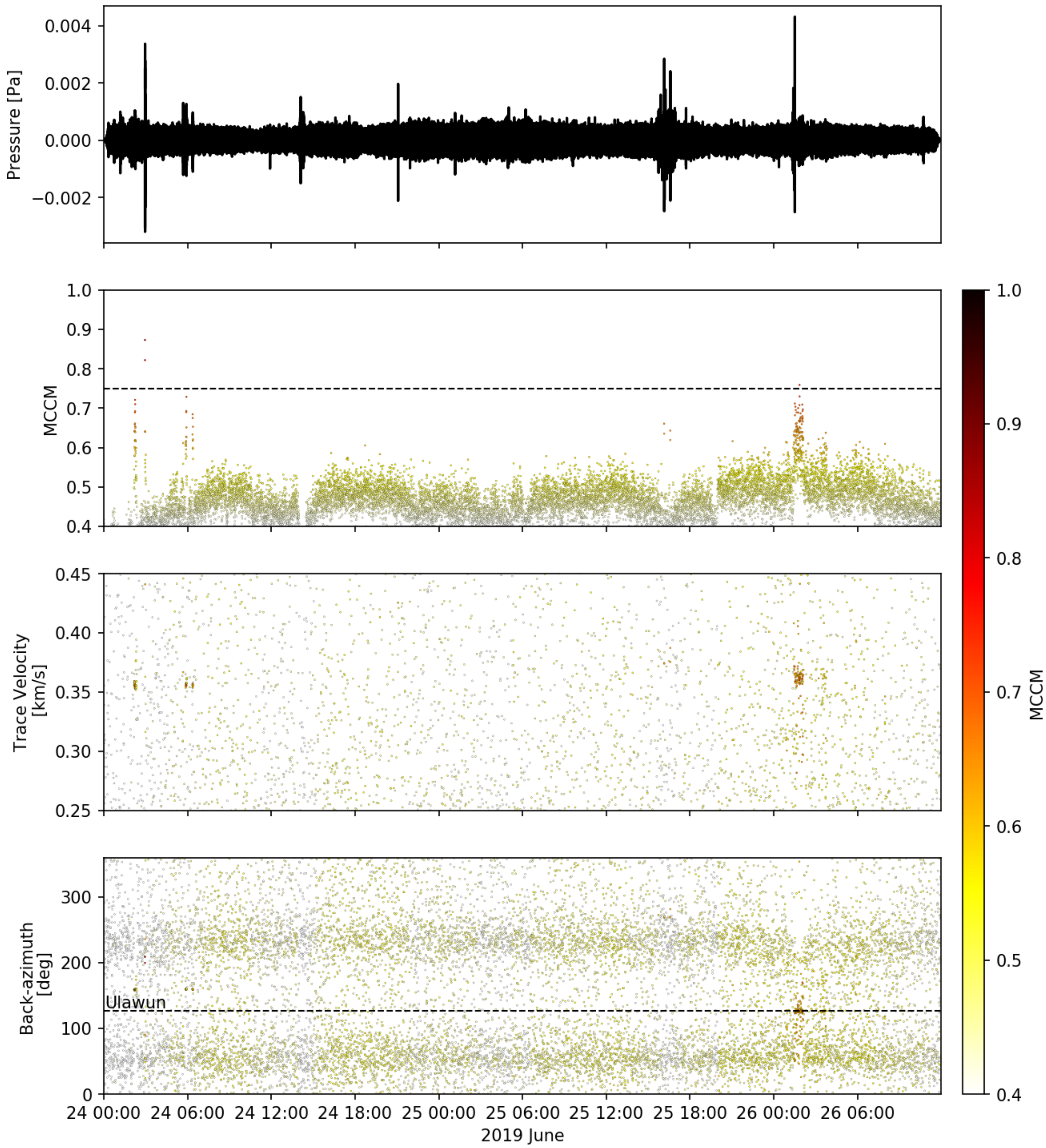

Sup. Fig. 4 - IS39 MdCCM array detection results Ulawun for 24 June at 00:00 to 26 June at 12:00 UTC, data filtered from 0.1 to 5.0 Hz. Top: Best beam of infrasound; 2nd: MCCM, mean cross correlation maximum; 3rd: Estimated trace velocity for each time window; Bottom: Estimated back-azimuth for each time window.

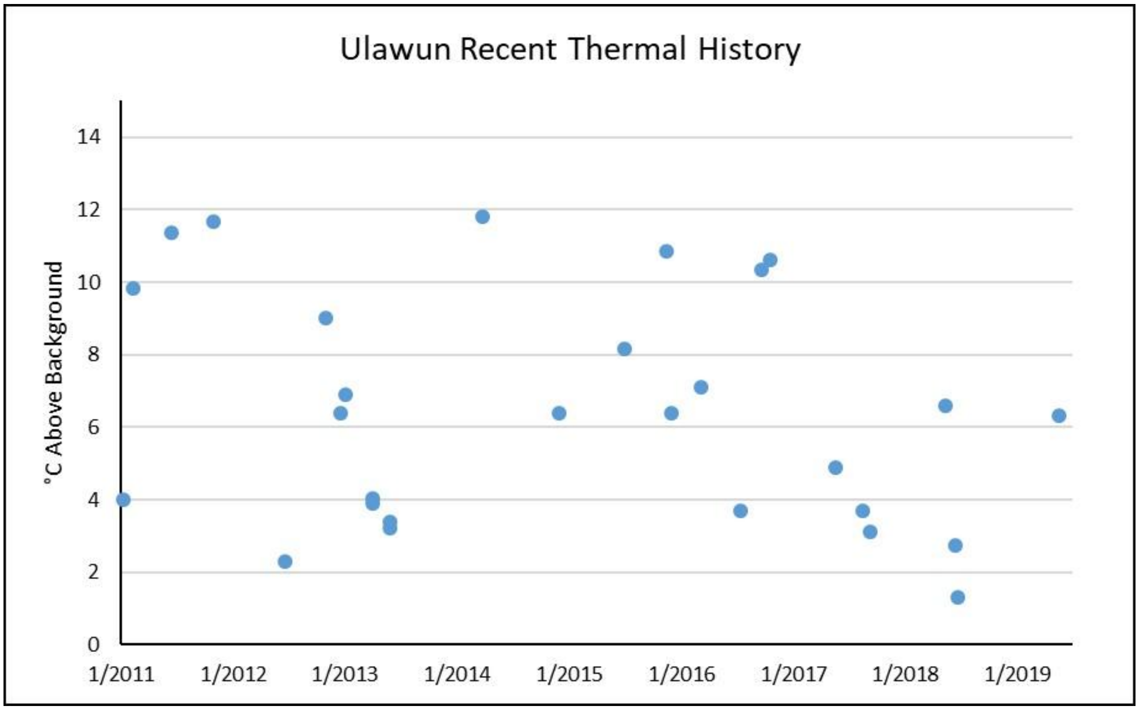

Sup. Fig. 5 - Ulawun thermal anomaly (deg. C above background) times series compiled from ASTER data.

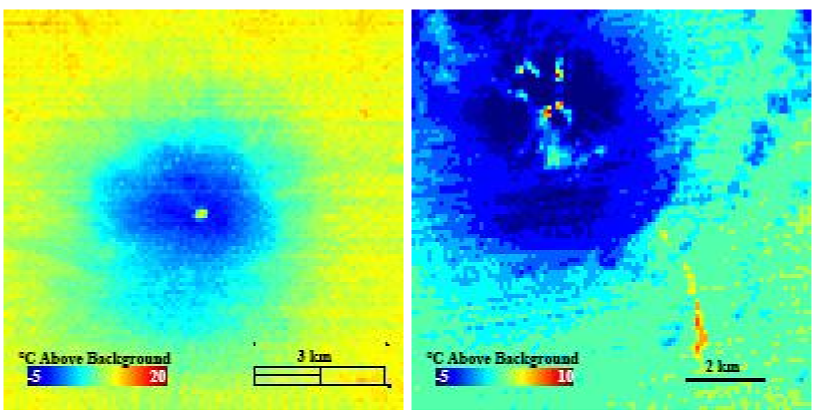

Sup. Fig. 6 - ASTER thermal imagery of Ulawun from 27 March 2014 (left) showing clear hot pixels at the summit and from 29 June 2019 (right) showing hot pixels at the summit and to the southeast.

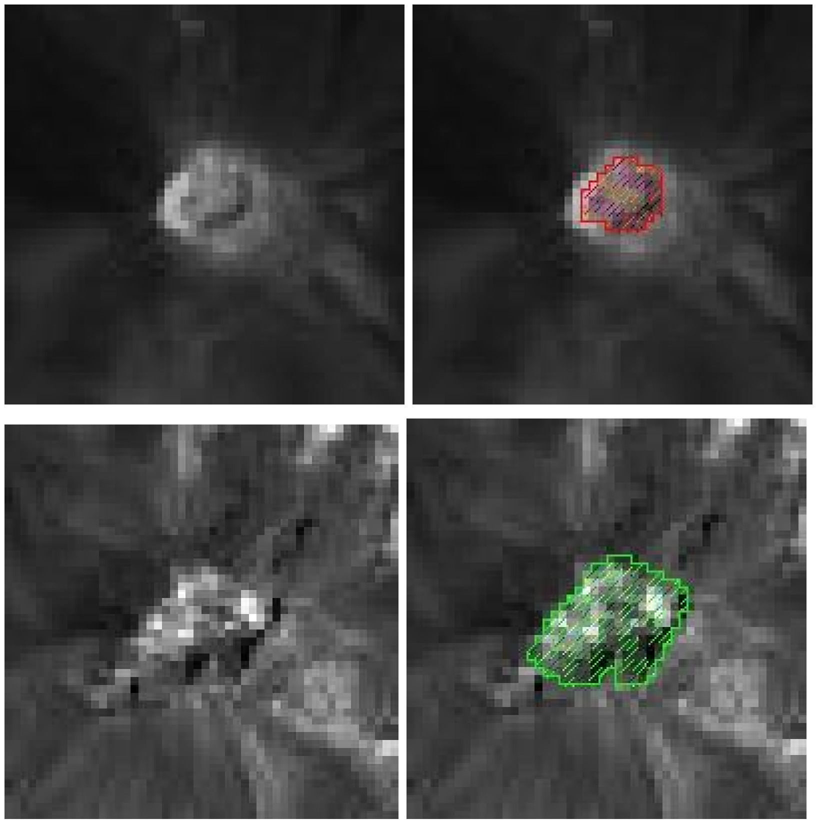

Sup. Fig. 7 - Ulawun crater area pre- and post-eruption. Sentinel-2 visible band data from 01 January 2018 (Row 1) and from 02 December 2019 (Row 1). Column 1 is the plain image and Column 2 has the crater shaded to illustrate the increase in area.

Sup. Table 1. Table of the parameter space used to select the initial source conditions in the Monte Carlo plume modelling.

Source Parameter	**Explored Range**
Velocity (m s^{-1})	25 - 250
Gas Mass Fraction	0.01 - 0.05
Temperature (K)	900 - 1400
Radius (m)	1 - 250